motifs or domains were found in the L-MPZ–specific extra region.

Developmental expression and localization of L-MPZ in the PNS–L-MPZ was enriched in the adult ScN myelin fraction and was translated from P0 mRNA. Because the expression of P0 protein is dramatically increased during early postnatal development, we next investigated the change in L-MPZ expression by stop codon readthrough during ScN development. L-MPZ and PNS myelin proteins (P0 and MBP-splice variants) were detected with western blotting. In myelin fractions obtained during the various developmental stages, L-MPZ was detected from P1, and expression increased with age, similar to the major PNS myelin proteins (Fig. 8A). Because myelinogenesis is active around P7 in the rat PNS, upregulation of L-MPZ in 5- to 7-day-old rat ScN myelin may be involved in the maturation of myelinated fibers.

To investigate the localization of L-MPZ in the PNS, double immunostaining of adult rat longitudinal ScN sections was performed using anti–L-MPZ (green) and anti-NF (red; Fig. 8B) antibodies. L-MPZ–positive signals were detected specifically in the myelin, which ensheathed NF-positive axons. Thus, L-MPZ is localized in the compact myelin of the PNS.

Cellular localization of L-MPZ and P0 in transfected HeLa cells–During myelination, P0 is targeted to the plasma membrane, and homophilic binding of extracellular Ig-like domains mediates intermembrane adhesion to form compact myelin (2). In the HeLa cell culture system, forcibly expressed P0 protein is localized to the plasma membrane, especially at sites of close apposition between two P0-expressing cells (26). To investigate the cellular localization of L-MPZ and P0, we performed double immunostaining of full-length P0 cDNA–transfected HeLa cells using anti–L-MPZ and anti-P0 antibodies. L-MPZ and P0 immunoreactivities were colocalized (Fig. 9A, first row,). While anti-L-MPZ can detect only L-MPZ, anti-P0 antibody detects mainly P0 but also slightly detects L-MPZ in western blot (Fig. 2A). Therefore, to confirm the individual distribution of P0 and L-MPZ in transfected cells, five types of mutant [deletion or frame-shift mutants to express only P0, deletion or replacement (Ala or Tyr) of P0 stop codon to express only L-MPZ-like molecules] were generated from full-length human P0 cDNA (Fig. 9B). The productions of these mutant molecules were confirmed by western blotting using anti-P0 or anti-L-MPZ antibodies (data not shown). In immunocytofluorescence, both individual P0 and L-MPZ-like molecules were detected in plasma membrane (Fig. 9A, second-6th rows). Especially, just like P0, L-MPZ-positive signals were accumulated at sites of cell-cell adhesion between two L-MPZ-like mutant-expressing cells (Fig. 9A, 4th-6th rows). These results indicate that L-MPZ may also contribute to cell adhesion.

DISCUSSION

In this study, we show that the highly antigenic 36-kDa neuropathy-associated protein, designated L-MPZ, is a novel isoform of P0 that contains an additional 63 aa at the C terminus of P0. This protein is probably produced by translational readthrough of the regular P0 stop codon, because L-MPZ was produced by the identical P0 mRNA in conjunction with P0 in transfected mammalian cells and because P0 peptides and peptides with the deduced aa sequence in the 3′UTR of P0 are both found with MS analysis of tryptic L-MPZ fragments. Stop codon readthrough was also shown by the great increase in L-MPZ synthesis with mammalian *in vitro* transcription/translation system in the presence of G418. P0 stop codon readthrough model mutants those only produced L-MPZ-like proteins were also synthesized by mammalian *in vitro* transcription/translation system. Like P0, L-MPZ was expressed during myelinogenesis, localized in compact myelin of the PNS, and accumulated at cell-cell adhesion sites in transfected cells, suggesting that L-MPZ is involved in the formation and/or maintenance of compact myelin, similar to P0. Because the L-MPZ–specific region contains an additional putative PKC phosphorylation site and is highly antigenic, L-MPZ may also have some unique roles in normal and pathological myelin conditions.

There was a high degree of homology at the aa level among the L-MPZ–specific coding regions in P0 mRNA from mammals and *X. laevis* (>80% identity in mammals and ~48% identity in *X. laevis*), but such homologies were not seen in zebrafish or shark P0 mRNA (data not shown). These findings suggest that evolutionarily, P0 may have acquired the L-MPZ–specific region by stop

codon readthrough after the evolutionary progression from amphibians. Regarding the CNS-specific myelin PLP and its alternatively spliced isoform DM20, it is believed that ancestral DM20 isoforms appeared in cartilaginous fish and evolved into PLP by the acquisition of the PLP-specific 35-aa region during the evolutionary progression from lobe-finned fish to amphibians (27). Phylogenetically, ancestral P0 is found in both the CNS and PNS from cartilaginous fish to some amphibians, and P0 became a PNS-specific protein after the evolution of amphibians (27, 28). Therefore, during the same course of evolution of PLP, acquisition of the L-MPZ–specific region may have been required for PNS-specific distribution and function in PNS myelin.

The main function of P0 is the formation and stabilization of the multilamellar membrane structure of compact myelin. Homophilic binding of extracellular Ig domains between face-to-face molecules is required for compaction. Our data suggest that L-MPZ may have the same extracellular structure (Fig. 7) that is involved in homophilic and/or L-MPZ/P0 heterophilic adhesion. PKC-mediated phosphorylation of specific residues (RSTK) in the cytoplasmic domain of P0 (Fig. 3B and Fig. 7) is necessary for P0-mediated adhesion, and alterations in this process can cause demyelinating neuropathy in humans (4). Because L-MPZ contains an additional predicted putative PKC phosphorylation site (RTSLK) in the cytoplasmic L-MPZ–specific region extending from the P0 C terminus (Fig. 3B and Fig. 7), phosphorylation of the L-MPZ–specific region may influence P0-mediated adhesion during myelin formation.

More than 120 mutations in the P0 gene have been identified in patients with hereditary neuropathies. These mutations and polymorphisms have been found in both the extracellular and intracellular regions (5; http://www.molgen.ua.ac.be/CMTMutations/). If L-MPZ has a similar structure as P0 and is involved in myelination, mutations in specific regions of L-MPZ may also modulate the adhesion and compaction of PNS myelin and cause cryptogenic neuropathies. Careful and large-scale screening of mutations or polymorphisms in the L-MPZ–specific region of the P0 gene may be important in understanding the spectrum of inherited neuropathies. The mechanism of anti–L-MPZ antibody production and its pathological role in neuropathies are still unclear. Since the epitope for the serum IgG of neuropathy patient is in the L-MPZ specific intracellular domain and highly antigenic, myelin debris generated by PNS demyelination may induce the production of anti–L-MPZ IgG in patients with neuropathies.

Stop codon readthrough is a process that increases the diversity of genomic information. This mechanism is well documented with respect to viruses (11), yeast (for review, 12), and *Drosophila* (13-15). Recently, enhancing stop codon readthrough artificially with aminoglycosides has been examined for the treatment of many inherited diseases caused by genes containing premature termination codons generated by mutations or abnormal splicing, such as cystic fibrosis and Duchenne muscular dystrophy (for review, 29). In contrast, so far, stop codon readthrough has not been reported under normal conditions in humans and other mammals. P0-related 36-kDa protein believed to be L-MPZ has been detected under normal conditions in human, bovine, rat, and mouse PNS (6-9). Because the aa sequence of the specific region of L-MPZ is highly conserved from frogs to humans (Fig. 3A), it is not simply due to an accidental misreading of the stop codon. Therefore, stop codon readthrough may be essential for modulating the function of regular-sized proteins in mammals. One possible process of stop codon readthrough at L-MPZ regular stop codon is natural nonsense supression by natural suppressor tRNA. A valiety of naturally occurring suppressor tRNAs were found in higher eukaryotes including mammals (for review, 30). Viruses use these suppressor tRNAs for the translational readthrough permitting the differential production of more than one polypeptide from a single gene in host eukaryotes. One of eukaryotic natural suppressor tRNA for UAG (amber) stop codon is $tRNA^{Tyr}$. If L-MPZ was produced in natural suppressor tRNA system, L-MPZ might be synthesized by such suppressor $tRNA^{Tyr}$, like one of mutant molecules produced by MutY_L-MPZ (Fig. 6A and Fig. 9A). In addition, nonsense suppression using suppressor tRNA is enhanced by G418 in mammalian culture cells (31). Since L-MPZ synthesis with *in vitro* transcription/translation was dramatically

increased by G418, L-MPZ may be produced by the suppression of the regular P0 stop codon. On the other hand, because G418 enhanced the production of L-MPZ *in vitro*, it will be necessary to consider the effects of aminoglycosides and other readthrough enhancer reagents on the normal readthrough of proteins *in vivo*.

Further analysis focusing on L-MPZ is now in progress to improve diagnosis and develop better treatment for peripheral neuropathies, as well as to determine its functional role in normal and pathological conditions of PNS myelin. Further, because this is the first report describing stop codon readthrough in a common mammalian protein, detailed analysis of L-MPZ expression may yield greater understanding of the mechanism of stop codon readthrough in mammals.

REFERENCES

1. Kirschner, D., Laurence, W., and Feltri, M. (2004) *Myelin Biology and Disorders*, Elsevier Academic Press, San Diego, CA, 523–545
2. Filbin, M. T., Walsh, F. S., Trapp, B. D., Pizzey, J. A., and Tennekoon. G. I. (1990) *Nature* **344**, 871–872
3. Wong, M. H., and Filbin, M. T. (1994) *J. Cell Biol.* **126**, 1089-1097
4. Xu, W., Shy, M., Kamholz, J., Elferink, L., Xu, G., Lilien, J., and Balsamo, J. (2001) *J. Cell Biol.* **155**, 439–446
5. Shy, M. E. (2006) *J. Neurol. Sci.* **242**, 55–66
6. Nobile-Orazio, E., Manfredini, E., Sgarzi, M., Spagnol, G., Allaria, S., Quadroni, M., and Scarlato, G. (1994) *J. Neuroimmunol.* **53**, 143–151
7. Meléndez-Vásquez, C. V., and Gregson, N. A. (1998) *J. Neuroimmunol.* **91**, 10–18
8. Ishida, K., Takeuchi, H., Takahashi, R., Yoshimura, K., Yamada, M., and Mizusawa, H. (2001) *J. Neurol. Sci.* **188**, 43–49
9. Favereaux, A., Lagueny, A., Vital, A., Schmitter, J.-M., Chaignepain, S., Ferrer, X., Labatut-Cazabat, I., Vital, C., and Petry, K. G. (2003) *J. Neurol. Neurosurg. Psychiatry.* **74**, 1262–1266
10. Besançon, R., Prost, A. L., Konecny, L., Latour, P., Petiot, P., Boutrand, L., Kopp, N., Mularoni, A., Chamba, G., and Vandenberghe, A. (1999) *FEBS Lett.* **457**, 339–342
11. Valle, R. P., Drugeon, G., Devignes-Morch, M. D., Legocki, A. B., and Haenni, A. L. (1992) *FEBS Lett.* **306**, 133–139
12. von der Haar, T., and Tuite, M. F. (2007) *Trends Microbiol.* **15**, 78–86
13. Steneberg, P., Englund, C., Kronhamn, J., Weaver, T. A., and Samakovlis, C. (1998) *Genes Dev.* **12**, 956–967
14. Steneberg, P., and Samakovlis, C. (2001) *EMBO Rep.* **2**, 593–597
15. Stark, A., et al. (2007) *Nature* **450**, 219–232
16. Hatfield, D., Thorgeirsson, S. S., Copeland, T. D., Oroszlan, S., and Bustin, M. (1988) *Biochemistry* **27**, 1179–1183
17. Chittum, H. S., Lane, W. S., Carlson, B. A., Roller, P. P., Lung, F. D., Lee, B. J., and Hatfield, D. L. (1998) *Biochemistry* **37**, 10866–10870
18. Yamaguchi, Y., Miyagi, Y., and Baba, H. (2008) *J. Neurosci. Res.* **86**, 755–765
19. Werner, H. B., Kuhlmann, K., Shen, S., Uecker, M., Schardt, A., Dimova, K., Orfaniotou, F., Dhaunchak, A., Brinkmann, B. G., Möbius, W., Guarente, L., Casaccia-Bonnefil, P., Jahn, O., and Nave, K.-A. (2007) *J. Neurosci.* **27**, 7717–7730
20. Freeze, H. H., and Kranz, C. (2010) *Curr. Protoc. Protein Sci.*, John Wiley & Sons, New York, NY, Unit12.4.
21. Yamaguchi, Y., Miyagi, Y., and Baba, H. (2008) J. Neurosci. Res. **86**, 766–775
22. Hayasaka, K., Nanao, K., Tahara, M., Sato, W., Takada, G., Miura, M., and Uyemura, K. (1991) *Biochem. Biophys. Res. Commun.* **180**, 515–518
23. Burke, J. F., and Mogg, A. E. (1985) *Nucleic Acids Res.* **13**, 6265–6272
24. Martin, R., Mogg, A. E., Heywood, L. A., Nitschke, L., and Burke, J. F. (1989) *Mol. Gen. Genet.*

217, 411–418
25. Manuvakhova, M., Keeling, K., and Bedwell, D. M. (2000) *RNA* **6**, 1044–1055
26. Doyle, J. P., Stempak, J. G., Cowin, P., Colman, D. R., and D'Urso, D. (1995) *J. Cell Biol.* **131**, 465–482
27. Yoshida, M., and Colman, D. R. (1996) *Neuron* **16**, 1115–1126
28. Rotenstein, L., Herath, K., Gould, R. M., and de Bellard, M. E. (2008) *Brain Behav. Evol.* **72**, 48–58
29. Linde, L., and Kerem, B. (2008) Trends Genet. **24**, 552–563
30. Beier, H., and Grimm, M. (2001) *Nucleic Acids Res.* **29**, 4767–4782
31. Phillips-Jones, M. K., Hill, L. S. J., Atkinson, J., and Martin, R. (1995) *Mol. Cell. Biol.* **15**, 6593–6600

Acknowledgements–We thank the patient for participating in this study and Dr. Kiyoshi Hayasaka for providing a human P0 cDNA clone. We also acknowledge the help of our laboratory members, especially Y. Naito, A. Nagata, T. Kikukawa, and R. Yamazaki.

FOOTNOTES

*This research was supported by a Japanese Health and Labor Sciences Research Grant for Research on Psychiatry and Neurological Diseases and Mental Health (H20-015), and the Promotion and Mutual Aid Corporation for Private Schools of Japan. The authors have no financial relationships and no conflicts of interest relevant to this article.

[1]To whom correspondence should be addressed: Department of Molecular Neurobiology, Tokyo University of Pharmacy and Life Sciences, Hachioji, Tokyo 192-0392, Japan
[2]Semel Institute for Neuroscience and Human Behavior, University of California at Los Angeles, Los Angeles, California 90095, [†]Deceased
[3]Department of Neurology and Geriatrics, Gifu University, Graduate School of Medicine, Gifu 501-1194, Japan

[4]The abbreviations used are: P0 or MPZ, myelin protein zero; L-MPZ, large myelin protein zero; PNS, peripheral nervous system; aa, amino acid; ScN, sciatic nerve; CIDP, chronic inflammatory demyelinating polyneuropathy; P, postnatal day; 2DE, two-dimensional gel electrophoresis; CTAB, cetyltrimethylammonium bromide; PNGase, Peptide:*N*-glycosidase; RT, room temperature; NDS, normal donkey serum; MBP, myelin basic protein; PLP, myelin proteolipid protein

FIGURE LEGENDS

FIGURE 1. Characterization of the 36-kDa protein detected by the serum IgG of a patient with CIDP. *A*, Western blotting of rat brain and ScN whole homogenates (10 μg protein). The 36-kDa band was detected in the ScN but not in the brain homogenate. *B* and *C*, Western blotting of the ScN fractions using the patient serum (Pt). The 36-kDa protein was detected in the membrane fraction (Mem) but not in the cytosolic fraction (Cyt; *B*) and was enriched in the myelin fraction (Myln; *C*). While β-actin and GAPDH (cytosolic and membrane associated proteins) were detected both cytosolic and membrane fractions, β-catenin (adherence junction marker) was extremely enriched in the membrane fraction (B). In the myelin fraction, MBP molecules (myelin marker) were enriched but not β-catenin, GAPDH, nor paxillin (focal contact marker) (C). *D*, After deglycosylation of N-linked sugar chains with PNGase F treatment of ScN whole homogenate, the relative molecular weight of the 36-kDa protein was shifted down in the same manner as P0. WH, whole homogenates; Nrml, negative control using normal human serum; M, marker.

FIGURE 2. Detection of the 36-kDa protein with anti-P0 antibody. *A*, Western blotting of ScN whole homogenates (10 μg protein). A band of the same size as the 36-kDa protein was recognized by anti-P0 (P0) antibody and by serum obtained from a patient with CIDP (Pt). *B* and *C*, 2DE western blotting of rat ScN whole homogenate using CTAB. Spots with identical positions (white arrows) were detected using anti-P0 (*B*, right) antibody and patient serum (*C*, right). The corresponding spots (white arrows) are shown on the colloidal silver–stained membranes (*B*, *C*, left panels). Anti-P0 antibody also recognized smaller bands than the P0 band, which were probably degradation products (*A* and *B*, right). Cntrl, negative control without primary antibody; M, marker.

FIGURE 3. The 36-kDa protein has evolutionarily conserved sequences derived from the 3′UTR of P0 mRNA. *A*, Sequence alignment of the deduced amino acid sequence of the region between the first and second stop codons in the 3′UTR of P0 cDNA of human, bovine, rat, mouse, and frog (*Xenopus laevis*). According to the degree of identity, amino acids are colored from light to dark gray. The sequence of this region is highly conserved. *B*, A summary of the identified tryptic peptides from the 36-kDa spot detected by CTAB-2DE following MS analysis (underlined sequences). Twelve peptides were identified in the entire P0 protein sequence (aa 30 to 248). Five peptides were identified in the predicted sequence from the 3′UTR of the P0 mRNA. The shaded box indicates the transmembrane region of P0. §, the protein kinase C (PKC)-mediated phosphorylation site in mature P0; ¶, the predicted PKC-mediated phosphorylation site in the 36-kDa–specific region; #, signal peptide cleavage site; *, stop codon.

FIGURE 4. Elimination of immunoreactivity for the 36-kDa band by specific peptides. *A*, The black bars depict the synthesized peptides with the additional 63-aa sequence: two peptides derived from the 63-aa sequence (P0-1 and P0-2), five partially overlapping peptides derived from P0-2 (P0-2-1 to -5), and a peptide used to produce the specific antibody in rabbit. A cysteine residue was added to the N terminus of the latter peptide for conjugation to keyhole limpet hemocyanin. *B* and *C*, Peptide absorption tests of the 36-kDa protein with immunoblots using serum IgG from a patient with CIDP. The immunoreactivity was completely blocked by the P0-2 peptide but not by P0-1 or a control non-related 21-aa peptide (NR; *B*). Only P0-2-4 absorbed the immunoreactivity of the 36-kDa band; P0-2-1, -2, -3, and -5 did not (*C*). The positive control (–) consisted of a sample containing no peptide. *D*, Western blotting using rabbit anti–L-MPZ produced by immunization with the synthetic peptide shown in *A*. The same 36-kDa band was recognized by the patient serum (Pt) and anti–L-MPZ (L-MPZ). The negative control (Cntrl) in each case had no primary antibody. Western blots of ScN whole homogenate had 10 μg protein/lane (*B* and *C*) or 5 μg protein/lane (*D*). M, marker.

FIGURE 5. Production of both L-MPZ and P0 from transfected human P0 cDNA. *A*, Western blots using anti-P0 antibody or a negative control without primary antibody (Cntrl) of lysates (10 μg) from NIH/3T3

cells transfected with human P0 (hP0) or a vector control (Vec). While non-specific band (arrowhead) was seen in each sample, P0 was detected only in cells transfected with human P0. *B*, Glycosylated and deglycosylated (by PNGase F) L-MPZ bands were detected in lysates from human P0–transfected NIH/3T3 cells. Cntrl, negative control without primary antibody. GAPDH, loading control. M, marker.

FIGURE 6. Synthesis of L-MPZ by *in vitro* transcription/translation using human P0 cDNA and G418. *A*, Autoradiography image of the *in vitro* transcription/translation reaction mixture (2 μl/lane; 100–200 μg endogenous protein) on SDS-PAGE gel (10.5%) using [^{35}S]methionine-labeling. P0 was detected in samples with the human P0 vector (hP0/pcDNA3; hP0) without G418. Increased translation of L-MPZ was detected in the hP0 sample with G418. All of three types of readthrough model mutant molecules as L-MPZ, deletion or replacement (Ala or Tyr) of P0 stop codon in hP0/pcDNA3 were detected (Del, MutA, MutY). *B*, Quantitative analysis of the relative ratio of P0 and L-MPZ bands intensity with or without G418. Significantly, P0 was decreased in half (**: < 0.0001) and L-MPZ was increased 5 times (*: < 0.001) by G418 treatment. Statistical analysis was performed using a two-way ANOVA (PRISM 5) followed by Bonferroni multiple comparison test of 4 samples. Ratio standard was intensity of one of P0 band in hP0 without G418. Vec, transcription/translation mixture using the control vector (pcDNA3); DNA(-), transcription/translation mixture without template DNA.

FIGURE 7. Schematic illustration of the structure of P0 and L-MPZ. Most of the L-MPZ structure is identical to that of P0. The cytoplasmic domain of P0 is highly basic (pI 11) and includes one PKC target motif. The L-MPZ–specific portion extends from the P0 C terminus, is also highly basic (pI 10), and contains one additional predicted PKC phosphorylation site in the antigenic region. Faint gray lines are drawed every 20 aa.

FIGURE 8. Production and localization of L-MPZ in the rat ScN. *A*, Western blot analysis of rat ScN whole homogenates (10 μg protein/lane) from P1, 3, 5, and 7 and adult rats. The primary antibodies were specific for L-MPZ, P0, and MBP-splice variants (MBPs; 14-, 17-, 18.5-, 21-kDa). Expression of L-MPZ began to increase at P3, in parallel with the expression patterns of the major PNS myelin proteins (P0 and MBP). Comparative control, β-actin (actin). *B*, Distribution of L-MPZ in the adult rat ScN. Double immunostaining of longitudinal ScN sections was performed using anti–L-MPZ (green) and anti-NF (red) antibodies. L-MPZ–positive signals were detected specifically in myelin that ensheathed NF-positive axons. Scale bar: 10 μm.

FIGURE 9. Localization of L-MPZ and P0 in HeLa cells transfected with human P0 cDNA and several mutants. *A*, Double immunostaining was performed using anti-P0 (first column, green) and anti–L-MPZ (second column, red) antibodies. DIC, differential interference contrast image (third column). Merge of first to third column images with DAPI-nuclear stain (blue) (forth column). L-MPZ–positive signals were colocalized with P0 signals (first row). Specific mutants expressing P0 (P0_3'del and P0_pnly) or L-MPZ-like molecules (del_, MutA_, MutY_L-MPZ) demonstrated the individual plasma membrane distribution of P0 or L-MPZ-like molecules. Just like P0, L-MPZ-positive signals were accumulated at cell-cell adhesion sites between two L-MPZ-like mutant-expressing cells (white arrows). Scale bar: 10 μm. *B*, Illustrations of the constructions of insert DNAs in pcDNA3 expression vectors.

Figure 1

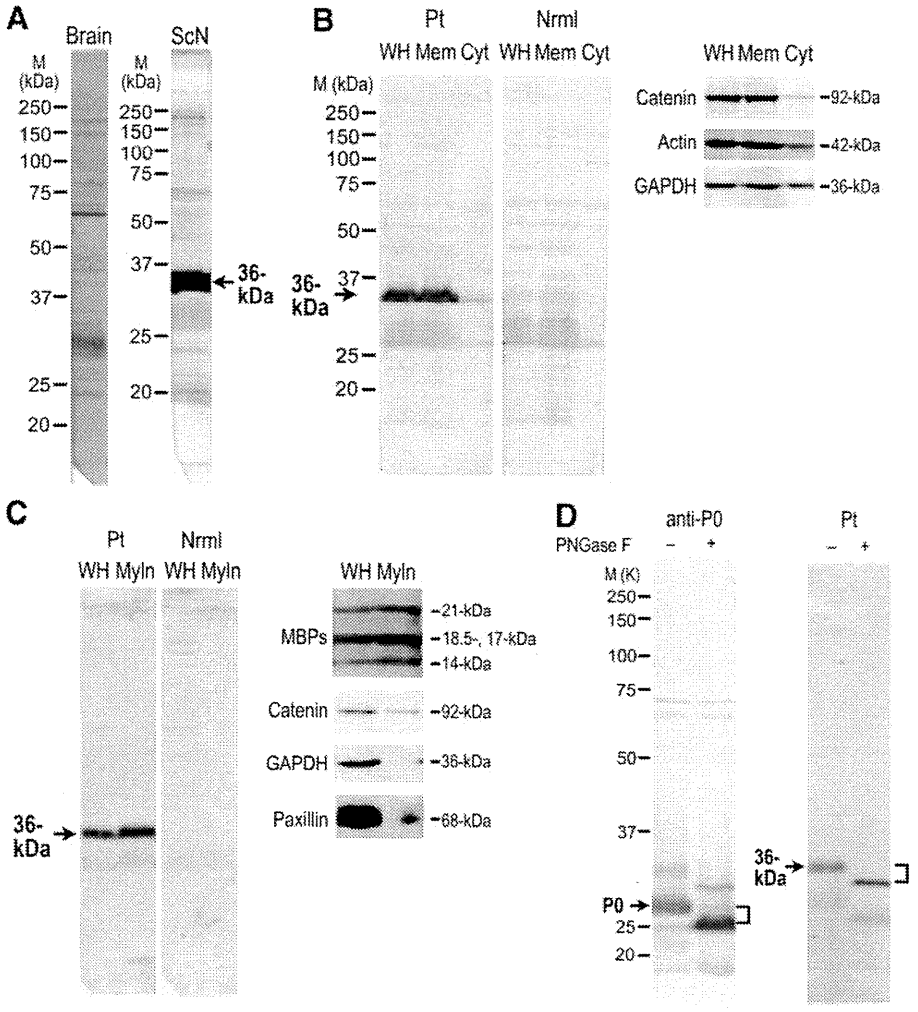
A
Brain
ScN
M (kDa)
250
150
100
75
50
37
25
20
36-kDa
B
Pt
Nrml
WH Mem Cyt
WH Mem Cyt
M (kDa)
36-kDa
Catenin
Actin
GAPDH
92-kDa
42-kDa
36-kDa
C
Pt
Nrml
WH Myln
WH Myln
WH Myln
36-kDa
MBPs
21-kDa
18.5-, 17-kDa
14-kDa
Catenin
92-kDa
GAPDH
36-kDa
Paxillin
68-kDa
D
anti-P0
Pt
PNGase F
M (K)
P0
36-kDa

Figure 2

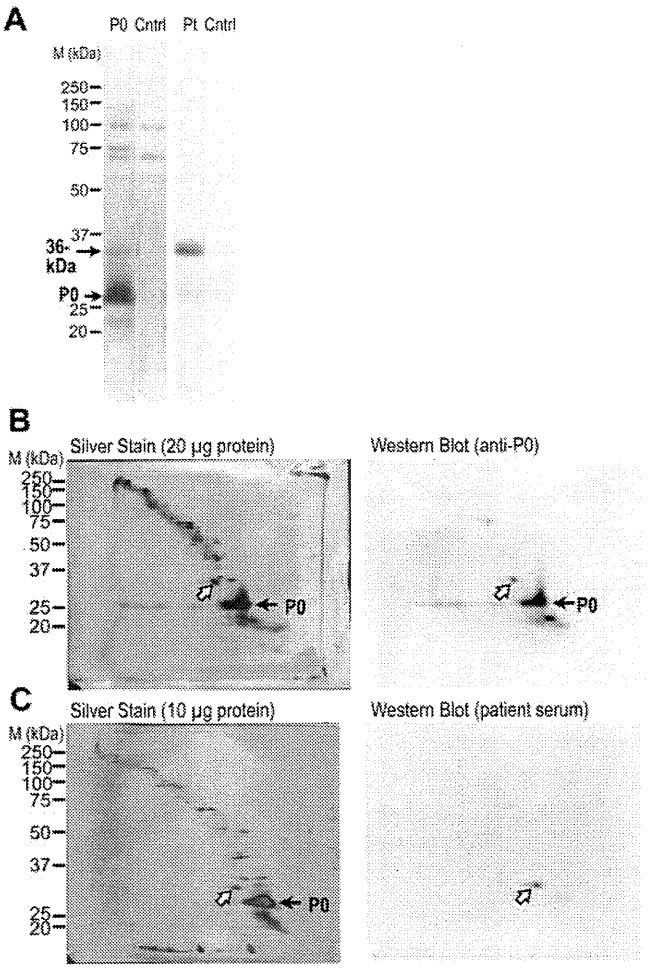
A
P0 Cntrl
Pt Cntrl
M (kDa)
250
150
100
75
50
37
36-
kDa
P0
25
20
B
Silver Stain (20 µg protein)
Western Blot (anti-P0)
M (kDa)
250
150
100
75
50
37
25
20
P0
P0
C
Silver Stain (10 µg protein)
Western Blot (patient serum)
M (kDa)
250
150
100
75
50
37
25
20
P0

Figure 3

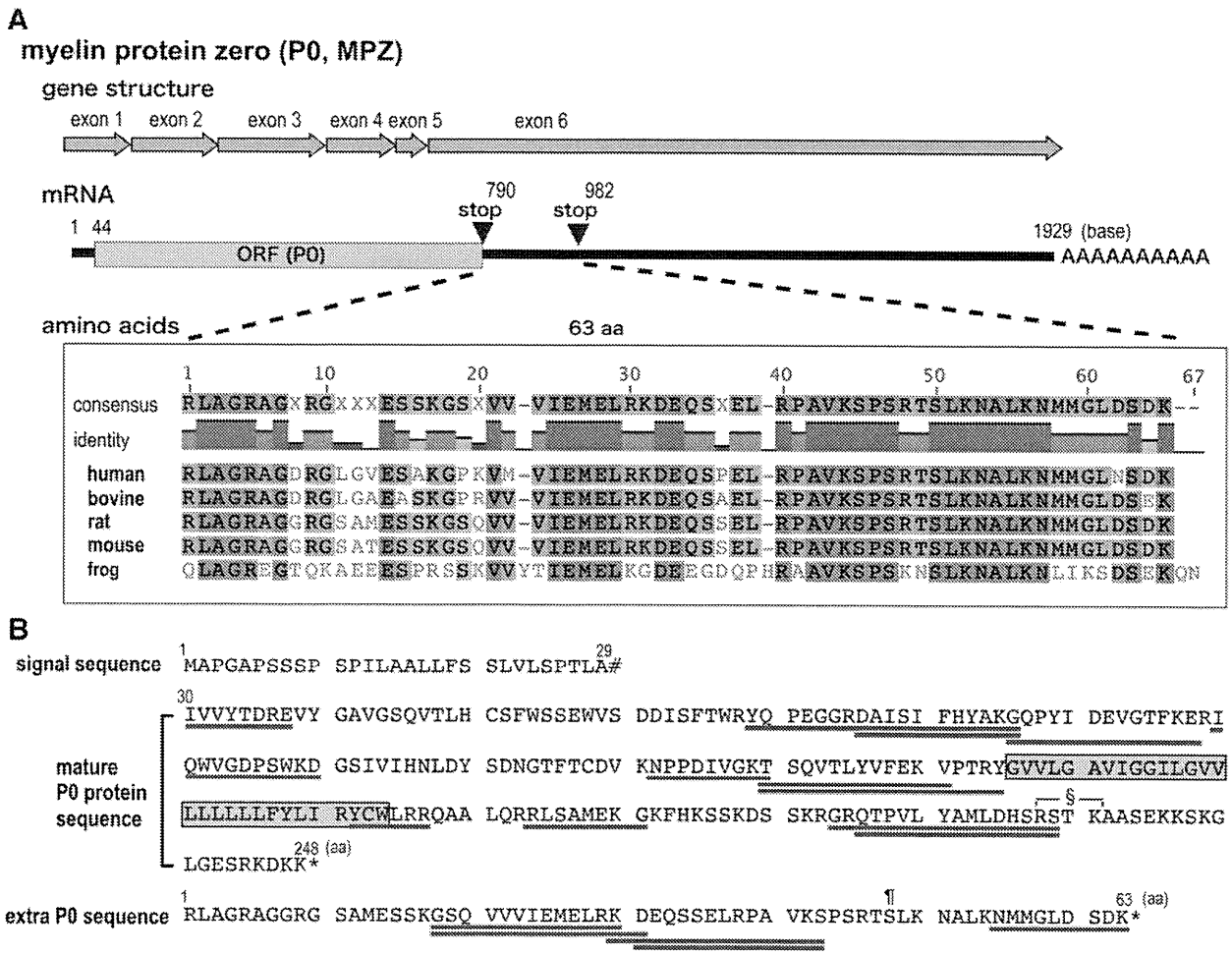
A
myelin protein zero (P0, MPZ)
gene structure
exon 1
exon 2
exon 3
exon 4
exon 5
exon 6
mRNA
1
44
ORF (P0)
790
stop
982
stop
1929 (base)
AAAAAAAAAA
amino acids
63 aa
consensus
identity
human
bovine
rat
mouse
frog
B
signal sequence
MAPGAPSSSP SPILAALLFS SLVLSPTLA#
mature P0 protein sequence
IVVYTDREVY GAVGSQVTLH CSFWSSEWVS DDISFTWRYQ PEGGRDAISI FHYAKGQPYI DEVGTFKERI
QWVGDPSWKD GSIVIHNLDY SDNGTFTCDV KNPPDIVGKT SQVTLYVFEK VPTRYGVVLG AVIGGILGVV
LLLLLLFYLI RYCWLRRQAA LQRRLSAMEK GKFHKSSKDS SKRGRQTPVL YAMLDHSRST KAASEKKSKG
LGESRKDKK*
248 (aa)
extra P0 sequence
RLAGRAGGRG SAMESSKGSQ VVVIEMELRK DEQSSELRPA VKSPSRTSLK NALKNMMGLD SDK*
63 (aa)

Figure 4

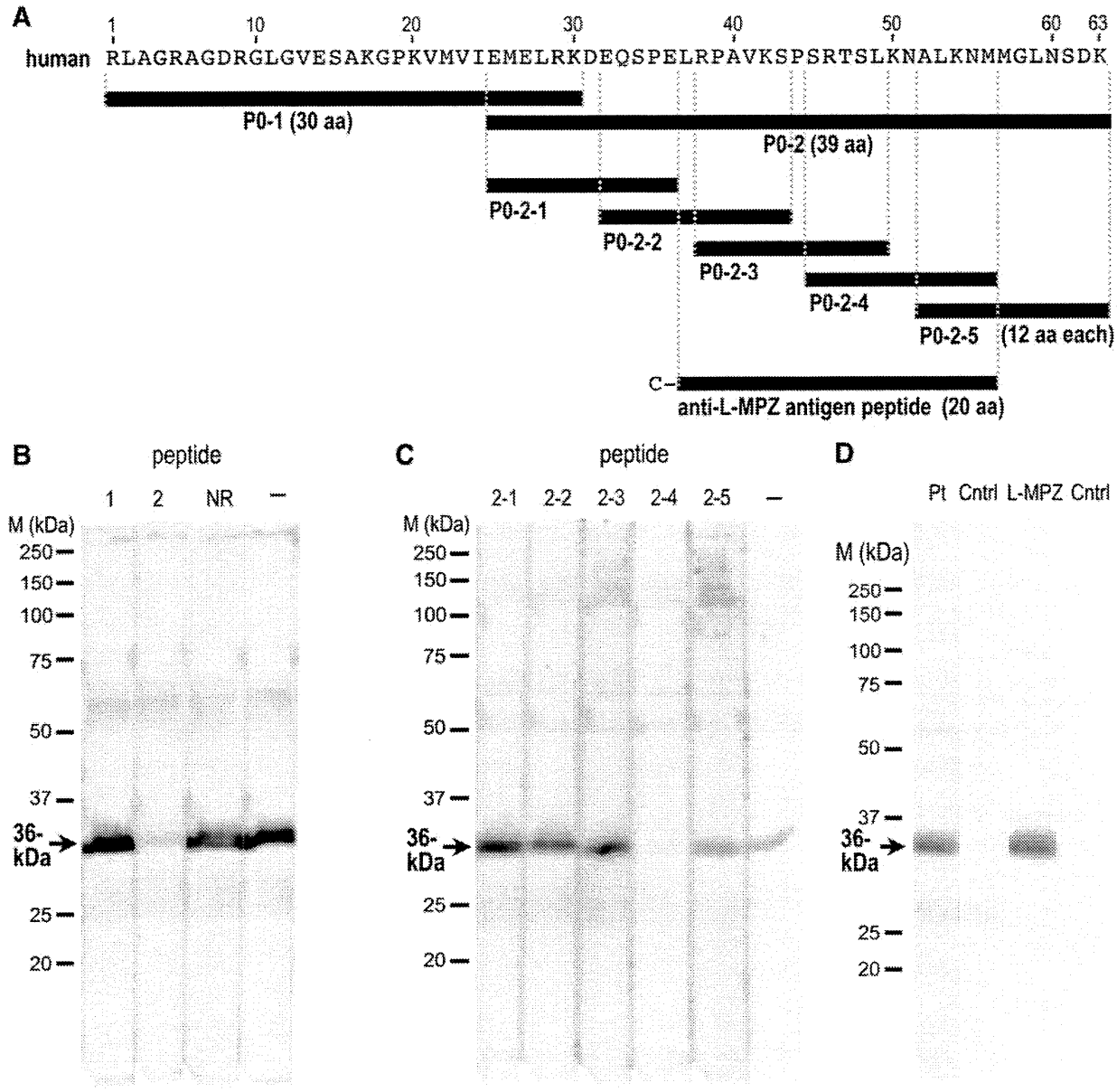
A
human RLAGRAGDRGLGVESAKGPKVMVIEMELRKDEQSPELRPAVKSPSRTSLKNALKNMMGLNSDK
P0-1 (30 aa)
P0-2 (39 aa)
P0-2-1
P0-2-2
P0-2-3
P0-2-4
P0-2-5 (12 aa each)
C
anti-L-MPZ antigen peptide (20 aa)
B
peptide
1 2 NR —
M (kDa)
250
150
100
75
50
37
36-kDa
25
20
C
peptide
2-1 2-2 2-3 2-4 2-5 —
M (kDa)
250
150
100
75
50
37
36-kDa
25
20
D
Pt Cntrl L-MPZ Cntrl
M (kDa)
250
150
100
75
50
37
36-kDa
25
20

Figure 5

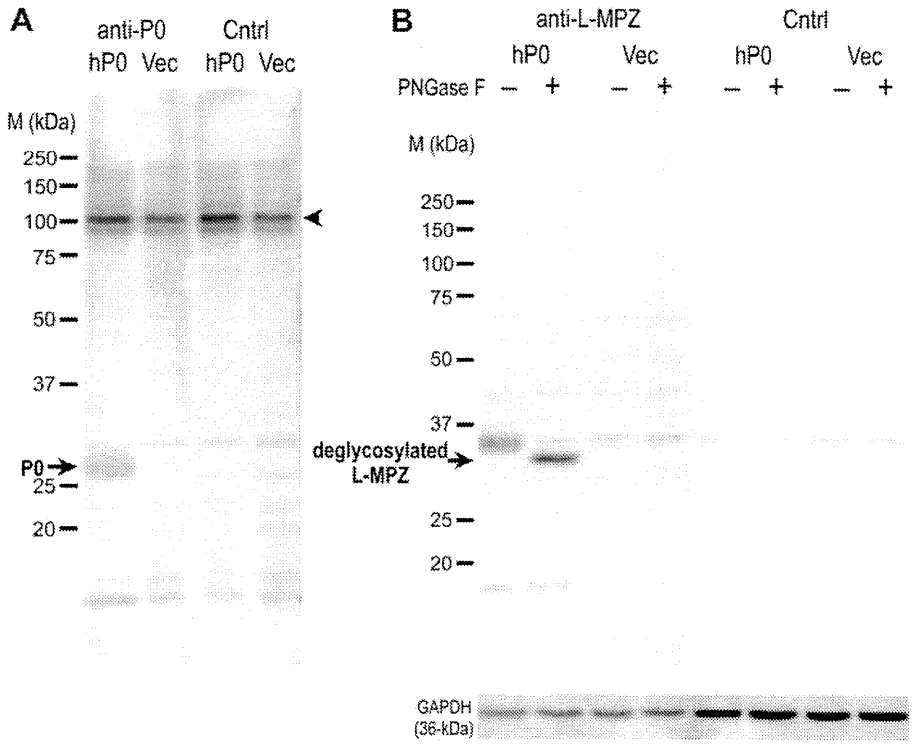
A
anti-P0
Cntrl
hP0 Vec hP0 Vec
M (kDa)
250
150
100
75
50
37
P0
25
20
B
anti-L-MPZ
Cntrl
hP0 Vec hP0 Vec
PNGase F – + – + – + – +
M (kDa)
250
150
100
75
50
37
deglycosylated L-MPZ
25
20
GAPDH (36-kDa)

Figure 6

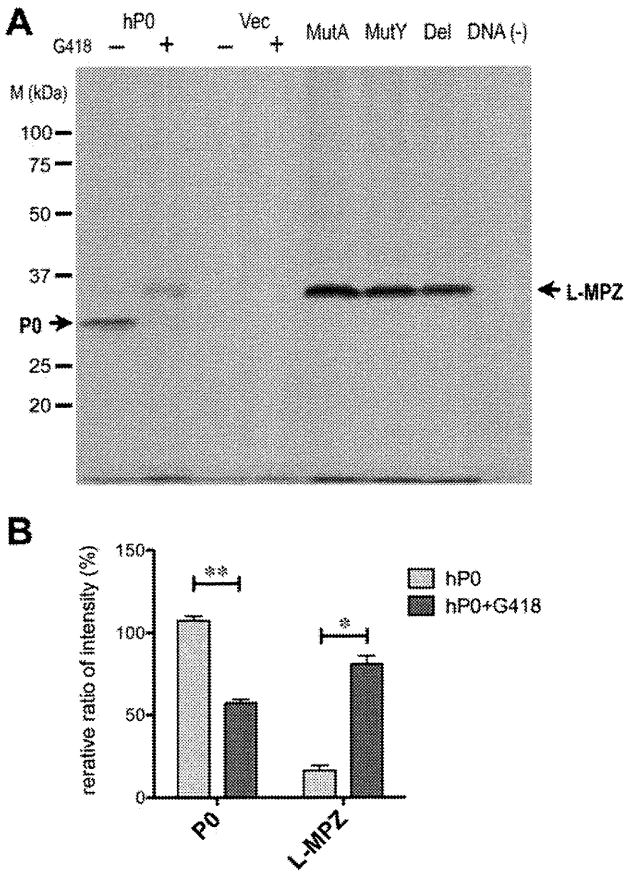
A
hP0
Vec
G418 – + – +
MutA MutY Del DNA (-)
M (kDa)
100
75
50
37
P0
25
20
L-MPZ
B
rerative ratio of intensity (%)
150
100
50
0
**
*
hP0
hP0+G418
P0
L-MPZ

Figure 7

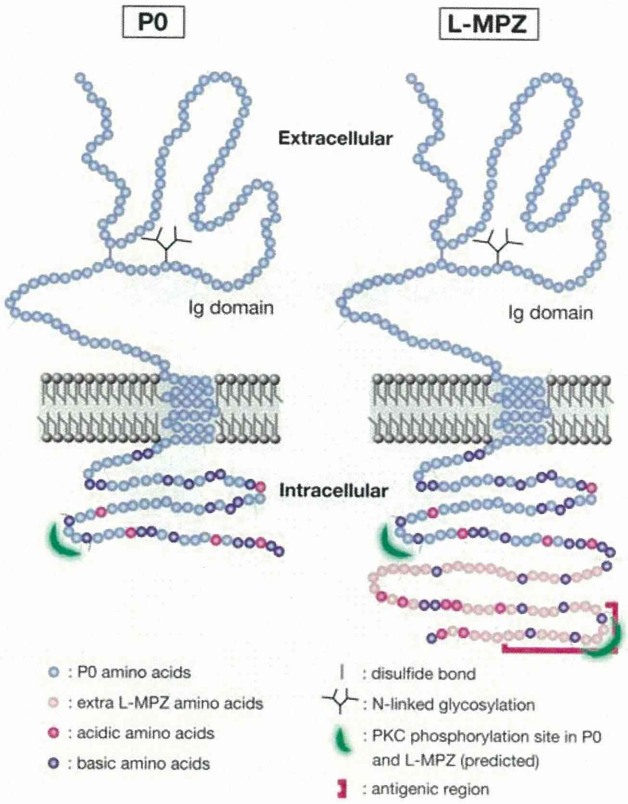
P0
L-MPZ
Extracellular
Ig domain
Ig domain
Intracellular
: P0 amino acids
: extra L-MPZ amino acids
: acidic amino acids
: basic amino acids
: disulfide bond
: N-linked glycosylation
: PKC phosphorylation site in P0 and L-MPZ (predicted)
: antigenic region

Figure 8

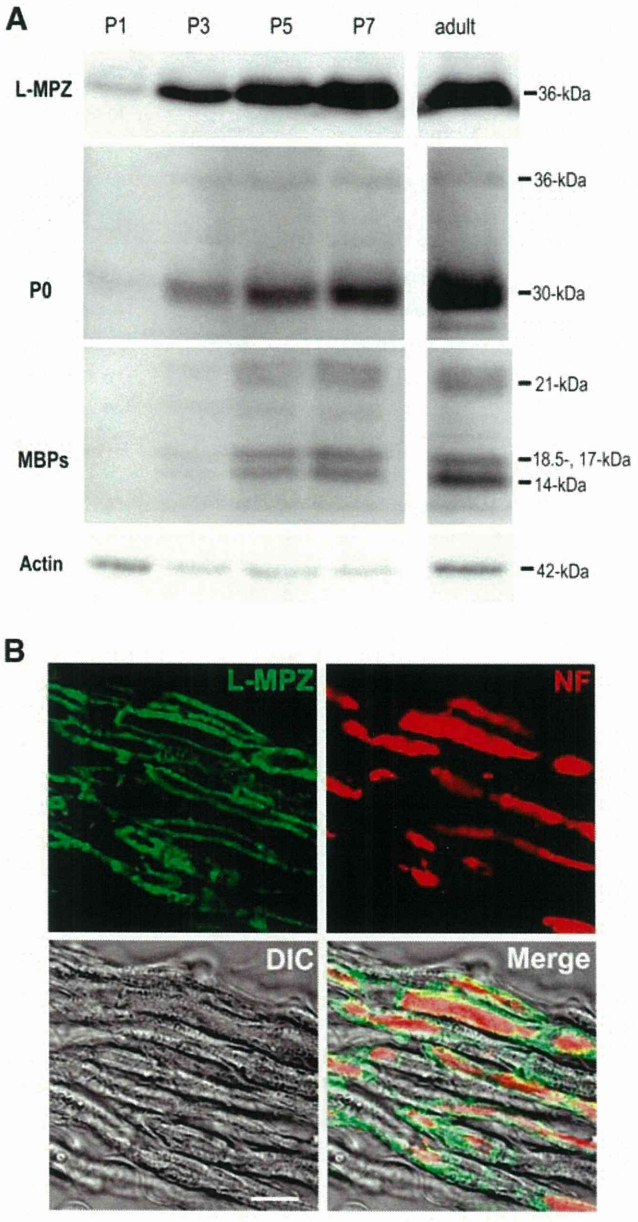
A
P1
P3
P5
P7
adult
L-MPZ
36-kDa
36-kDa
P0
30-kDa
21-kDa
MBPs
18.5-, 17-kDa
14-kDa
Actin
42-kDa
B
L-MPZ
NF
DIC
Merge

Figure 9

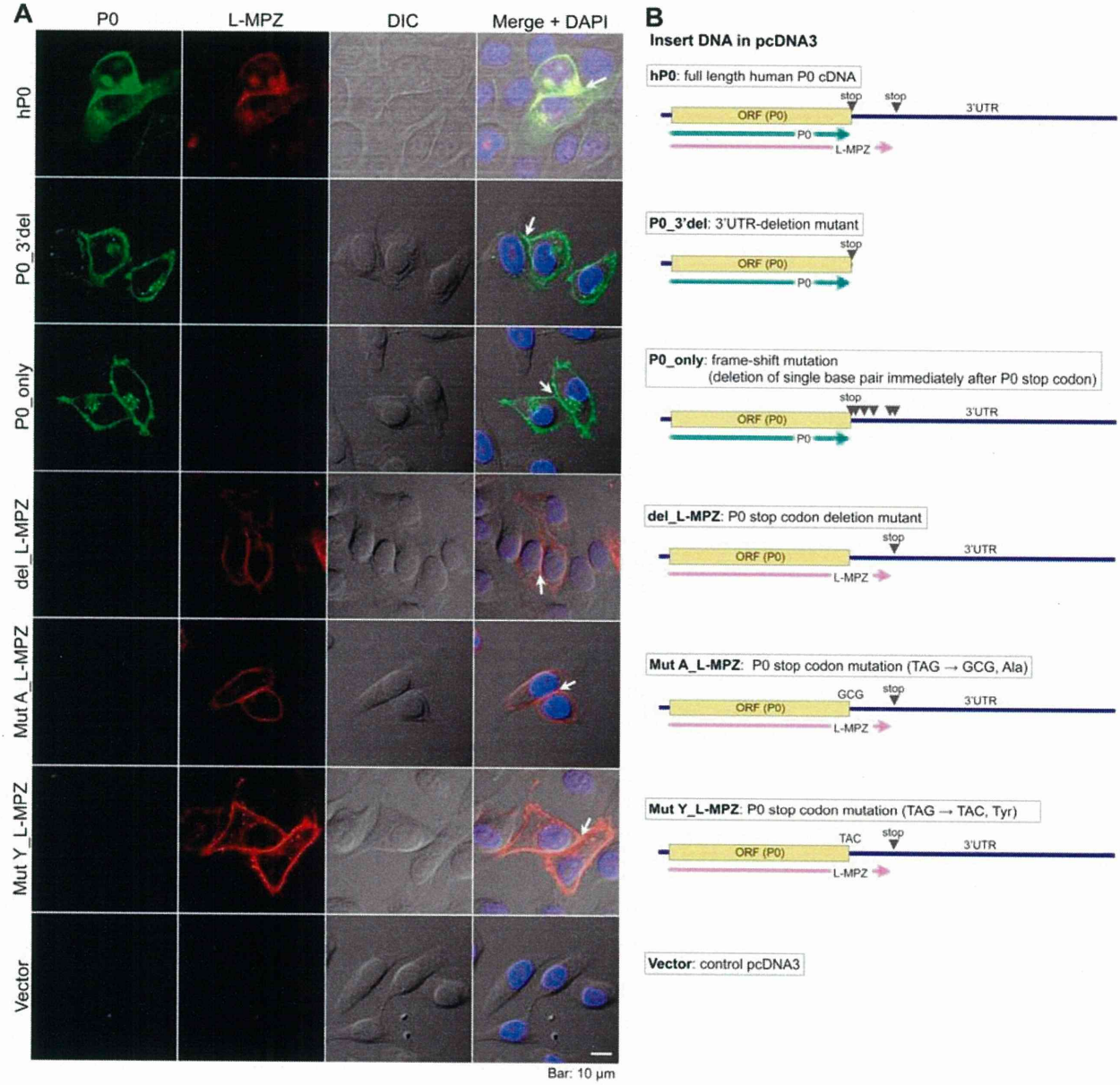
A
P0
L-MPZ
DIC
Merge + DAPI
hP0
P0_3'del
P0_only
del_L-MPZ
Mut A_L-MPZ
Mut Y_L-MPZ
Vector
Bar: 10 µm
B
Insert DNA in pcDNA3
hP0: full length human P0 cDNA
stop
stop
3'UTR
ORF (P0)
P0
L-MPZ
P0_3'del: 3'UTR-deletion mutant
P0_only: frame-shift mutation
(deletion of single base pair immediately after P0 stop codon)
del_L-MPZ: P0 stop codon deletion mutant
Mut A_L-MPZ: P0 stop codon mutation (TAG → GCG, Ala)
GCG
Mut Y_L-MPZ: P0 stop codon mutation (TAG → TAC, Tyr)
TAC
Vector: control pcDNA3